ACS APPLIED MATERIALS & INTERFACES

Research Article

www.acsami.org

Polyethylenimine-Grafted Cellulose Nanofibril Aerogels as Versatile Vehicles for Drug Delivery

Jiangqi Zhao,[†] Canhui Lu,[†] Xu He,[†] Xiaofang Zhang,[†] Wei Zhang,*[,†] and Ximu Zhang*[,‡,#]

[†]State Key Laboratory of Polymer Materials Engineering, Polymer Research Institute at Sichuan University, No. 24 South Section 1, Yihuan Road, Chengdu 610065, China

[‡]State Key Laboratory of Oral Disease, West China Hospital of Stomatology, Sichuan University, Chengdu 610041, China

[#]Department of Preventive Dentistry, West China Hospital of Stomatology, Sichuan University, Chengdu 610041, China

Supporting Information

ABSTRACT: Aerogels from polyethylenimine-grafted cellulose nanofibrils (CNFs-PEI) were developed for the first time as a novel drug delivery system. The morphology and structure of the CNFs before and after chemical modification were characterized by scanning electron microscopy (SEM), Fourier transform infrared spectroscopy (FTIR), and X-ray photoelectron spectroscopy (XPS). Water-soluble sodium salicylate (NaSA) was used as a model drug for the investigation of drug loading and release performance. The CNFs-PEI aerogels exhibited a high drug loading capability (287.39 mg/g), and the drug adsorption process could be well described by Langmuir isotherm and pseudo-second-order kinetics models. Drug release experiments demonstrated a sustained and controlled release behavior of the aerogels highly dependent on pH and temperature. This process followed quite well the pseudo-second-order release kinetics. Owing to the unique pH- and temperature-responsiveness together with their excellent biodegradability and biocompatibility, the CNFs-PEI aerogels were very promising as a new generation of controlled drug delivery carriers, offering simple and safe alternatives to the conventional systems from synthetic polymers.

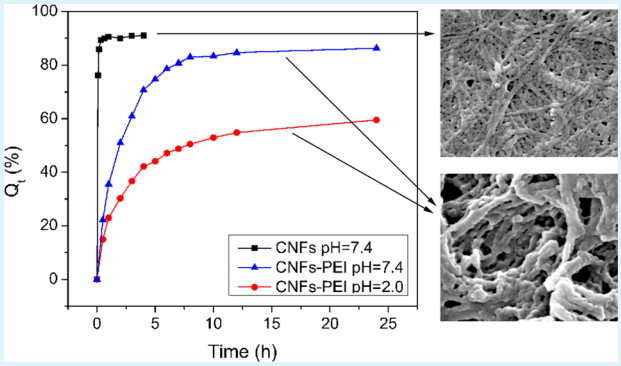

KEYWORDS: *aerogel, cellulose nanofibrils (CNFs), controlled release, drug delivery, polyethylenimine (PEI)*

INTRODUCTION

Conventional drug formulations have many adverse effects, including gastrointestinal or renal side effects.[1−3] In addition, most nonsteroidal anti-inflammatory drugs have short plasma elimination half-life (2−4 h) and must be administered in multiple daily doses to maintain therapeutic blood levels.[4] There has been a significant interest in the development of drug delivery systems, as they can provide a relatively steady release rate, reduce toxicity, optimize the drug therapeutics, and improve patient compliance and convenience.[4,5] The rate of drug delivery, the intensity, and the duration of drug action have been the subject of much multidisciplinary research.[6,7] These factors tend to be influenced by external conditions such as pH and temperature[8,9]

A number of polymers have been developed to achieve controlled release of drugs.[5] However, most of them, such as PE, PP, and PDMS, are synthetic and nonbiodegradable.[5,10,11] Currently, the use of natural polysaccharides or their derivatives is attractive and regarded as key formulation ingredients for the engineering of modified drug delivery systems because of their stability, availability, renewability, and low toxicity.[12] Cellulose is the most abundant natural polysaccharide in the world,[13] possessing nontoxic, renewable, biodegradable, and biocompatible characteristics.[14,15] In addition to the above-mentioned advantages of cellulose, nanocellulose, particularly cellulose nanofibrils (CNFs), exhibit many other unique characteristics, such as very large specific surface area,[16] high strength and stiffness,[17] ease for chemical modification,[18,19] and the ability to form highly porous mesh.[20] As a result, CNFs have gotten wide attention in various research areas and also been studied as excipient in formulation of the pharmaceutical dosage forms.[21−23]

Common drug delivery systems include ion exchange resins, films,[24,25] microspheres, gels, and so on.[26,27] There is growing interest in aerogels as a special class of highly porous materials with biomedical and pharmaceutical applications because of their open pore structure and high surface area.[12] However, efforts in this regard have been mainly focused on silica or carbon aerogels.[28,29] The polysaccharide-based aerogels have been developing very fast in drug delivery research in the past several years, giving rise to enhanced drug bioavailability and drug loading capacity.[27,30] In particular, CNFs hydrogels can be

Received: November 3, 2014
Accepted: January 6, 2015
Published: January 6, 2015

DOI: 10.1021/am507601m
ACS Appl. Mater. Interfaces 2015, 7, 2607−2615

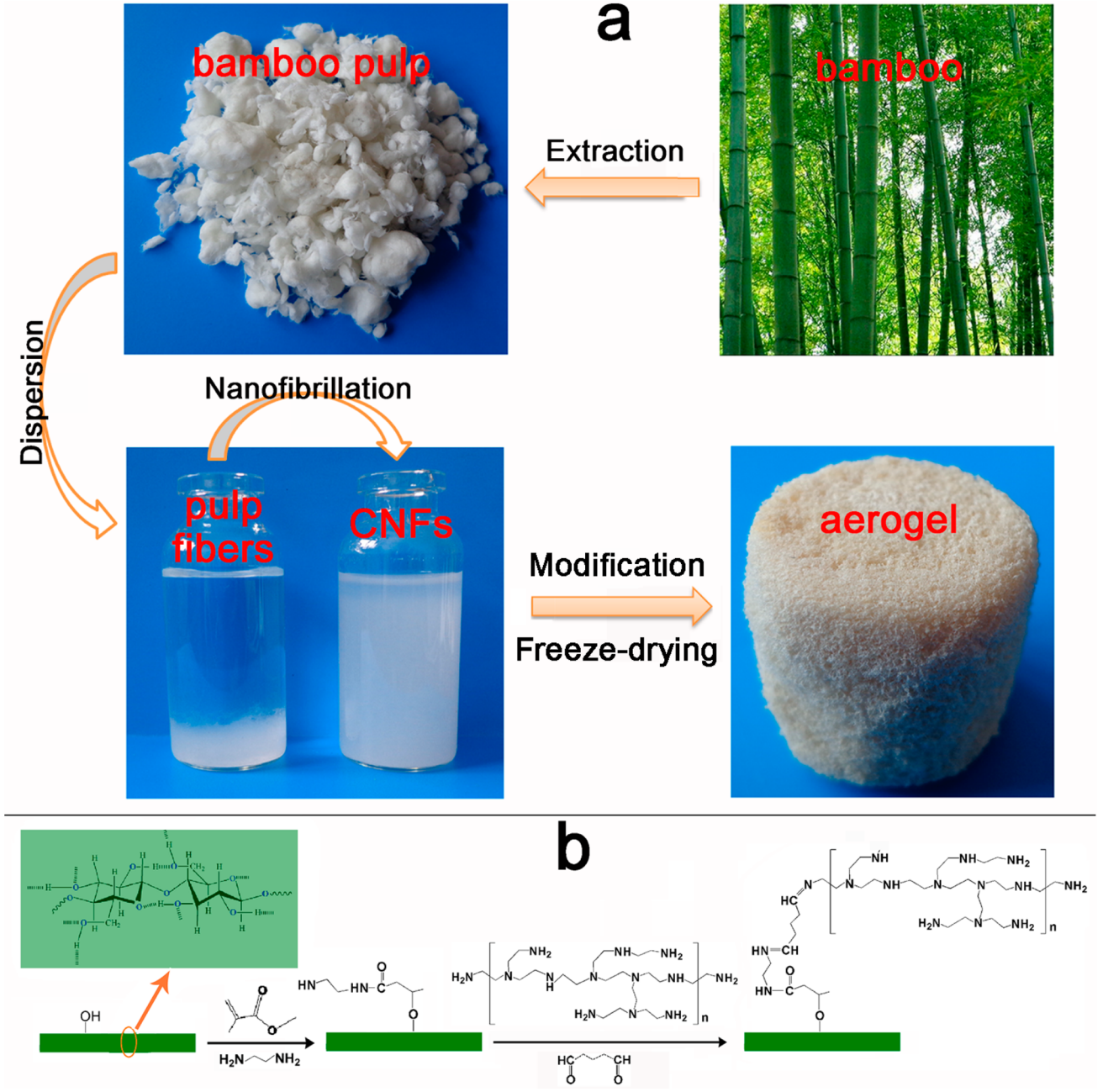

Figure 1. Schematic illustration of (a) the preparation process of the CNFs-PEI aerogels and (b) the reaction mechanism of the grafting process.

easily transformed into aerogels via freeze-drying.[21,27] The unique structure of CNFs aerogels provides them a broad range of applications such as templates,[31] adsorbents,[32] and drug delivery.[12,27] However, for pristine cellulose, the drug loading capability is very low. Thus, chemical modification of cellulose becomes an important step to improve its practical usefulness in drug delivery.[33,34] It is also important to note that surface modification of materials can dramatically influence their release profile and bioavailability of the entrapped drug.[12] Amide groups are commonly selected for conjugating drugs to polymers because they can bind a variety of negatively charged drug molecules.[35] In early work, polyethylenimine (PEI), which bears a large number of primary and secondary amine groups on the molecules, has demonstrated excellent performance in drug delivery.[36−38]

The objective of this study was to develop a new class of drug delivery systems based on CNFs. To this end, the PEI-grafted CNFs (CNFs-PEI) were synthesized and subsequently converted into aerogels through freeze-drying. The morphology and structure of the materials were characterized by SEM, FTIR, and XPS. Sodium salicylate (NaSA), a widely used medicine for curing diseases such as wound healing,[39] diabetes,[40] arthritis,[41] and cancer treatment,[42,43] was adopted as a model drug for investigating the drug loading and release performance of the CNFs-PEI aerogel.

MATERIALS AND METHODS

Materials. Never-dried moso bamboo pulp (Figure 1a) was supplied by Yongfeng Paper Co., Ltd. (Sichuan, China). Its cellulose content was higher than 93% as reported by the supplier. A branched polyethylenimine (PEI, average M_w of 25000) was purchased from

DOI: 10.1021/am507601m
ACS Appl. Mater. Interfaces 2015, 7, 2607−2615

Sigma–Aldrich. Sodium salicylate and other chemicals were of analytical grade and supplied by Chengdu Kelong Chemicals Co., Ltd. (Sichuan, China).

Preparation of CNFs. The bamboo pulp was dispersed in distilled water at a solid concentration of 1 wt %. A horn-type ultrasonic generator (JY99-IIDN, Scientz, China) was used to treat the suspension (500 mL) at an output power of 1200 W for 30 min. The suspension was then diluted to the concentration of 0.5 wt % with distilled water. Finally, a high shear homogenizer (T18, IKA, Germany) was used to isolate CNFs at a rotation speed of 20000 rpm for 1 h. The obtained CNFs could be well dispersed in water, as shown in Figure 1a.

Preparation of CNFs-PEI Aerogel. A schematic depiction of the grafting process of PEI on CNFs is presented in Figure 1b. First, amino groups were introduced onto the surface of CNFs. For a typical reaction, 1 g of CNFs was dispersed in 100 mL of methanol under nitrogen atmosphere and 1.5 g of methyl methacrylate was slowly added with cerium ammonium nitrate (6 mM) as an initiator. This free radical reaction was conducted at room temperature for 3 h under magnetic stirring. The products were washed three times with methanol and incubated with 1.5 g of ethylenediamine in a methanol solution. The transesterification reaction lasted for 24 h at 60 °C under magnetic stirring. The as prepared amino-modified CNFs (CNFs-NH_2) were purified through repeated methanol washing. The CNFs-PEI was synthesized as follows: 2 g of CNFs-NH_2 was immersed in 100 mL of PEI solution in methanol (2 wt % PEI) for 24 h under magnetic stirring at room temperature. After that, it was transferred into 200 mL of 1 wt % glutaraldehyde solution and stirred for 30 min. To ensure thorough removal of methanol and glutaraldehyde, the resulting product was washed repeatedly with distilled water and finally separated through centrifugation. The obtained CNFs-PEI was redispersed in water at a solid concentration of about 1 wt %. The suspensions were rapidly frozen in liquid nitrogen (−196 °C) and placed in a freeze-drying chamber (FD-1A-50, Biocool, China). The freeze-drying process was maintained at −30 °C for 72 h. The final product was a three-dimensional aerogel in light-yellow color (Figure 1a).

Material Characterization. The morphologies of cellulose fibers and CNFs-PEI were observed using scanning electron microscopy (SEM, Inspect F 50, FEI, USA). Cross-sectional features of the aerogel before and after drug release were also examined. The specific surface area of the aerogels was determined by nitrogen adsorption using Quantachrome NovaWin instrument (USA) and Brunauer–Emmett–Teller (BET) analysis method.[44] The chemical structure of samples was characterized by FTIR and XPS, respectively. FTIR analysis was performed using a Nicolet 560 FTIR spectrometer (Nicolet, USA). All spectra were scanned from 4000 to 500 cm^{-1} at a resolution of 2 cm^{-1}. XPS spectra were recorded on a Kratos XASAM 800 spectrometer (Kratos analysis, UK) with an Al Kα X-ray source (1486.6 eV) and an X-ray beam of around 1 mm.

Drug Loading Studies. The CNFs-PEI aerogels as well as the neat CNFs aerogels were loaded with NaSA through static adsorption. The stock solution was prepared by dissolving the NaSA in twice distilled water. Working solutions of the desired concentrations were obtained by successive dilutions. A series of batch adsorption experiments were conducted to investigate the effects of pH and reaction time and to estimate the maximum adsorption capacity. The pH dependent adsorption behaviors were studied in the pH range from 1 to 6 adjusted by 0.1 mol/L HCl or NaOH solutions. The aerogels were added into NaSA aqueous solutions for drug adsorption at ambient temperature for 24 h. The drug loading of aerogels could be determined from the initial and final drug concentrations of the solutions. The effect of initial drug concentration (NaSA concentration from 5 to 3000 mg/L) on the adsorption performance was studied at pH = 3 for 24 h. Meanwhile, the effect of contact time was examined up to 24 h at pH = 3.

Drug Release Studies. The effect of pH on the drug release behavior was evaluated. Drug-loaded aerogels were suspended in simulated gastric fluid (SGF, 0.2% NaCl, pH = 2) and simulated intestinal fluid (SIF, 0.05 mol/L, NaH_2PO_4, pH = 7.4) without protease, maintaining at 37 °C under a paddle rotation speed of 50 rpm. To study the temperature dependent drug release behavior, the experiments were performed at different temperatures (20, 37, and 50 °C). Samples (5 mL) were withdrawn at specific intervals, and the incubation solution was replenished with 5 mL of SIF or SGF after each sampling. The NaSA concentration were measured from the maximum absorbance at 295 nm using a UV–vis spectrophotometer (UV-1600, MAPADA, China).[27] The cumulative percentage of drug release was calculated and the mean of three determinations was used in data analysis.

RESULTS AND DISCUSSION

Characterization of The Materials. The morphologies of the materials were observed by SEM. Parts a and b of Figure 2 show the SEM images of pristine bamboo pulp fibers and the as-prepared CNFs, respectively. It was clear that the cellulose fibers had been almost completely disintegrated into CNFs after the combined physical treatments. The diameters of the pristine bamboo pulp fibers were about 10 μm, whereas most of the CNFs had diameters in the range of 20–40 nm. Figure 2c showed the morphology of CNFs-PEI. These modified CNFs exhibited obviously thicker fiber diameters (50–150 nm) as compared with the precursor CNFs. The appearance of thicker fibrils is consistent with the successful grafting of PEI. The cross-sectional feature of CNFs-PEI aerogel is shown in Figure 2d. The aerogel possessed a highly porous structure consisting of a network of interconnected nanofibrils and nanofibril bundles, part of which had formed sheet-like structure. This is normal for freeze-dried aerogels. The growth of ice crystals will push CNFs into sheets during the freezing process.[31,45] Because of the nano dimension of CNFs and the unique porous structure, the CNFs-PEI aerogel had a much higher BET surface area (79 m^2/g) than that of pristine bamboo pulp fibers (0.8 m^2/g), which accounted for enhanced adsorption properties.[46] It was noteworthy that the porous morphology of the CNFs-PEI aerogel was not affected after drug release, as shown in Figure S1 in the Supporting Information.

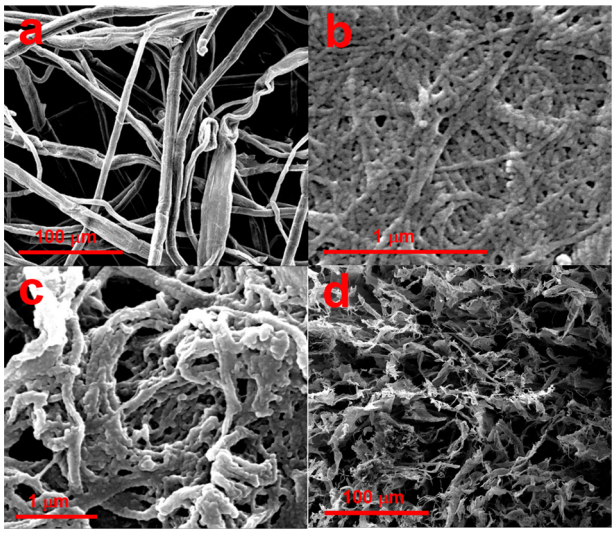

Figure 2. SEM images of the bamboo pulp fibers before (a) and after (b) the combined physical treatments, (c) the as-prepared CNFs-PEI, and (d) the cross-section of the aerogel.

FTIR spectra (Figure 3) were collected to elucidate the chemical structure changes after surface modification of CNFs. Compared with the CNFs sample, the most relevant difference

DOI: 10.1021/am507601m
ACS Appl. Mater. Interfaces 2015, 7, 2607–2615

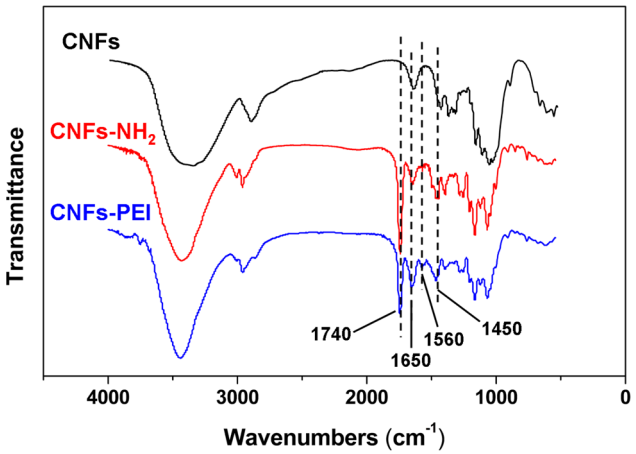

Figure 3. FTIR spectra for bamboo CNFs, the as-prepared CNFs-NH_2, and the as-prepared CNFs-PEI.

in the FTIR spectra of CNFs-NH_2 and CNFs-PEI is the appearance of bands at 1740, 1650, 1560, and 1450 cm^{-1}. The absorption peak at 1740 cm^{-1} could be ascribed to the C═O stretching of the ester groups.[47] It revealed that methyl methacrylate had been grafted to CNFs. In the meantime, it also suggested the reaction between esters and ethylenediamine was incomplete for this solid–liquid reaction.[47] The absorption at 1650, 1560, and 1450 cm^{-1} were the characteristic peaks of amide bond and amino group.[48−50] The relative intensities of these peaks in CNFs-PEI significantly increased as compared with that of CNFs-NH_2, indicative of the successful grafting of PEI onto CNFs.

XPS is a powerful analytical technique to study the surface chemical composition of materials.[51] With this tool, the chemical composition changes of CNFs during surface modification could be revealed. As shown in Figure 4, the XPS spectrum of CNFs did not display any signals in the N_{1s} region, indicating there was no nitrogen element presented in the CNFs.[49,52] However, for the CNFs-NH_2 spectrum, there was also no N_{1s} signal. This is possibly due to the very low content of amino groups on CNFs-NH_2, which outranged the detecting limits of the instrument. In contrast, a strong peak at 399.3 eV appeared in the CNFs-PEI spectrum. The nitrogen content of CNFs-PEI was estimated to be as high as 4.24%, further confirming the successful grafting of PEI to the CNFs' surface. The presence of these abundant amino groups were desirable for an enhanced drug loading performance of CNFs-PEI aerogels.[12]

Drug Loading Studies. *Influence of Solution pH.* pH is one of the most important factors that can affect the adsorption behavior remarkably.[36] In this study, a pH range of 1−6 was selected to investigate the drug loading capacities under these conditions and the results were presented in Figure 5. As

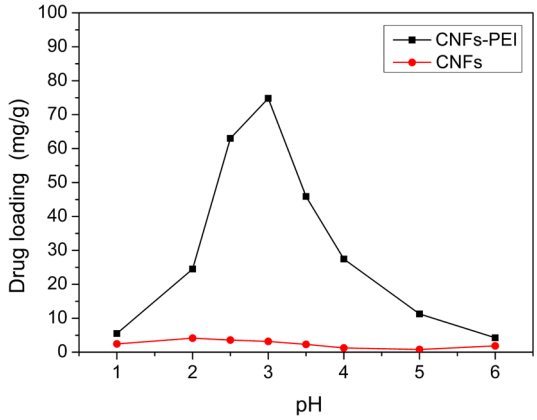

Figure 5. Effect of pH on drug loading of CNFs-PEI aerogels.

expected, the CNFs-PEI showed distinctly higher drug loading capacity than CNFs throughout the pH range. For CNFs-PEI, when pH increased from 1 to 3, the drug loading increased rapidly and reached the maximum at pH 3. In this condition, the drug loading of CNFs-PEI was as high as 78.00 mg/g, more than 20 times that of CNFs. However, when pH was over 3, the drug loading decreased sharply with the increase of solution pH. This phenomenon could be ascribed to the different interactions between the surface charges of the adsorbents and the SA^- at different pH. The $-NH_2$ groups on the surface of CNFs-PEI varied in form at different pH levels.[36] Under acidic conditions, amino groups could be protonated to form positively charged sites, e.g., $-NH_3^+$ groups.[36] The electrostatic attraction between $-NH_3^+$ and SA^- gave rise to the increase of drug loading. The bell-shaped curve for CNFs-PEI in Figure 5 could be predicted based on pK_a values with Henderson−Hasselbalch equations[53,54]

$$\mathrm{pH} = \mathrm{p}K_{a_1} + \log \frac{[SA^-]}{[SA]} \quad (1)$$

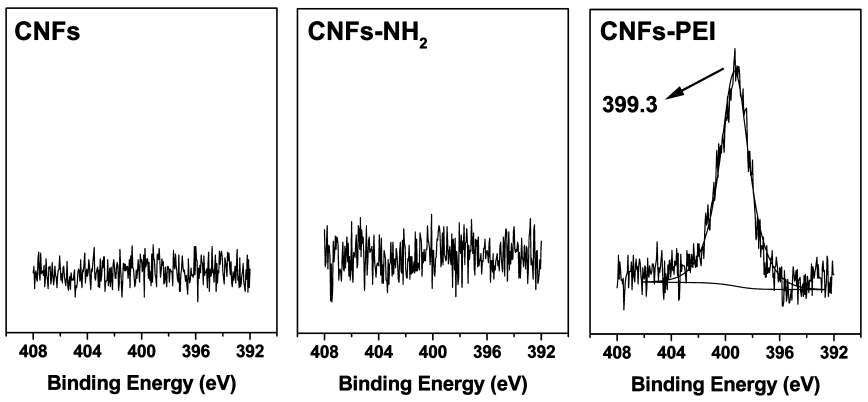

Figure 4. XPS N1s core-level spectra of bamboo CNFs, the as-prepared CNFs-NH_2, and the as-prepared CNFs-PEI.

DOI: 10.1021/am507601m
ACS Appl. Mater. Interfaces 2015, 7, 2607−2615

$$\mathrm{pH} = \mathrm{p}K_{a_2} + \log \frac{[\mathrm{NH_2}]}{[\mathrm{NH_3}^+]} \quad (2)$$

When pH increased, the concentration of H^+ in the fluid decreased. It became more difficult for $-NH_2$ to be protonated and thus the NH_3^+ concentration decreased, leading to a lower drug loading. The pK_{a1} for SA was about 3.[55] At pH 3, the amino groups on the CNFs-PEI (pK_{a2} = 8.8 for PEI)[56] could be extensively protonated to bear positive charges. Meanwhile, a half of SA was presented in its ionic form of SA^- in solution, leading to the maximum drug loading at pH 3. However, when pH further decreased (pH < pK_{a1}), the SA^- concentration would be reduced rapidly. Most of them would be transformed into salicylic acid, which could not be electrostatically attracted by the $-NH_3^+$ groups.[57] As a result, the drug loading capacities also decreased.

Adsorption Isotherms. Adsorption isotherms describe how adsorbates interact with adsorbents and are important in optimizing the use of the latter. Similarly, adsorption isotherms have great significance to elucidate the relationship between the drug carriers and drugs. The equilibrium adsorption capacity was obtained using eq 3. The equilibrium adsorption data were fitted with the Langmuir model (eq 4)[58] and the Freundlich model (eq 5),[36] respectively:

$$q_e = \frac{(C_o - C_e) \times V}{m} \quad (3)$$

$$q_e = \frac{q_m K_L C_e}{1 + K_L X C_e} \quad (4)$$

$$q_e = K_F C_e^{1/n} \quad (5)$$

where C_o and C_e (mg/L) are the initial and equilibrium concentrations of NaSA in solution, V (L) is the volume of drug solution, m (g) is the dry mass of adsorbents, q_e (mg/g) is the equilibrium adsorption capacity, q_m (mg/g) is the maximum adsorption capacity, K_L and K_F are constants for Langmuir and Freundlich isotherms, respectively, and n is a Freundlich constant relating to adsorption intensity of the adsorbents.[59]

The acquired data and the fitting curves are shown in Figure 6, and those important parameters obtained from fitting were presented in Table 1. Compared with the Freundlich isotherm, the Langmuir isotherm could better describe the adsorption behaviors with a correlation coefficient $R^2 > 0.95$, indicating a monolayer adsorption of NaSA onto the CNFs-PEI surface.[58,60]

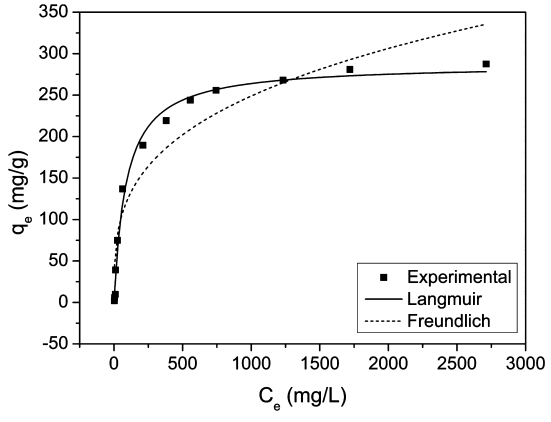

Figure 6. Two adsorption isotherms for CNFs-PEI aerogels.

Table 1. Isotherm Constants for the Adsorption of NaSA onto the CNFs-PEI Aerogel

	Langmuir model			Freundlich model		
sample	q_m (mg/g)	K_L (L/mg)	R^2	n	K_F (L/mg)	R^2
CNFs-PEI	287.39	0.011	0.9895	0.299	31.471	0.8991

The maximum adsorption capacity of NaSA calculated from the Langmuir isotherm was 287.39 mg/g for CNFs-PEI aerogel, representing an effective drug carrier.

Kinetics Studies. The adsorption kinetics was studied to manifest the adsorption rate of NaSA onto the CNFs-PEI aerogel as well as the rate controlled equilibrium time. The experimental data was analyzed using the pseudo-second-order equation (eq 6) as follows[61]

$$\frac{1}{q_r} = \frac{1}{k_2 q_e^2} + \left(\frac{1}{q_e}\right) t \quad (6)$$

where q_e is the adsorption capacity (mg/g) at equilibrium, q_t (mg/g) is the adsorption capacity at time t, and k_2 (g/mg·h) is the rate constant of pseudo-second-order adsorption.

The adsorption behavior of CNFs-PEI on NaSA as a function of contacting time is shown in Figure 7a. At the initial stage, the adsorption of NaSA was very fast and then gradually reached the equilibrium in 2 h. The experimental data and the linear fitting are shown in Figure 7b. The correlation coefficient and some other important parameters obtained from the fitting are presented in Table 2. The plots appeared in good linearity with a high correlation coefficient (R^2 = 0.9990), and the theoretical q_e value (279.33 mg/g) was very close to the experimental data (278.54 mg/g). These results indicated the pseudo-second-order kinetics model described quite well the experiment data.

Drug Release Studies. *Effect of pH on Drug Release.* The time dependence of NaSA release from the drug-loaded carriers in two different solutions, SGF (pH = 2) and SIF (pH = 7.4), was investigated. The obtained data was plotted in Figure 8. Compared with CNFs, the drug release rate of CNFs-PEI significantly slowed down. For CNFs aerogel, the drug release generally reached the equilibrium in 20 min. On the contrast, approximately 10 h was needed for CNFs-PEI to reach the equilibrium, suggesting the surface grafting with PEI was very effective to render CNFs aerogel sustained drug release performance. Because the CNFs-PEI aerogels prolonged drug release time effectively (improved from 20 min to 10 h with several tens times), and which were superior to many other drug deliveries,[27,30,62] which demonstrate the high potential of CNFs-PEI aerogels for pharmaceutical applications. The NaSA release rate from drug carriers could be analyzed using pseudo-second-order equation (eq 7):[63]

$$\frac{t}{Q_t} = \frac{1}{k_2 Q_e^2} + \left(\frac{1}{Q_e}\right) t \quad (7)$$

where Q_e (%) is the cumulative release at equilibrium, Q_t (%) is the cumulative release at time t, and k_2 (h^{-1}) is the rate constant of pseudo-second-order equation.

The graphical representations and the corresponding parameters calculated from the kinetics model are shown in Figure 8b and Table 3, respectively. The NaSA release from all the drug carriers followed the pseudo-second-order kinetics

DOI: 10.1021/am507601m
ACS Appl. Mater. Interfaces 2015, 7, 2607−2615

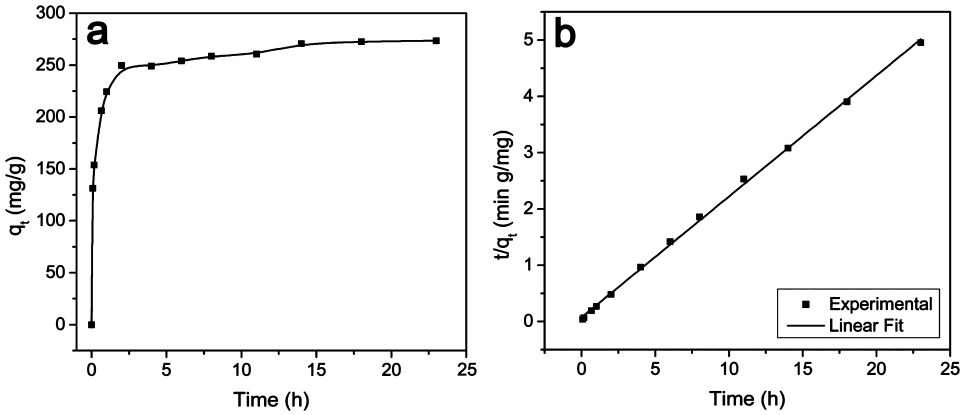

Figure 7. (a) Adsorption curves for CNFs-PEI aerogel and (b) linear fitting of NaSA adsorption data using the pseudo-second-order equation.

Table 2. Adsorption Kinetics Constants for the Adsorption of NaSA onto the CNFs-PEI Aerogel

		pseudo-second-order kinetics model		
sample	$q_{e,exp}$ (mg/g)	k_2 (g/mg·h)	$q_{e,cal}$ (mg/g)	R^2
CNFs-PEI	278.54	0.011	279.33	0.9990

Table 3. NaSA Release Kinetics from the Drug-Loaded CNFs and CNFs-PEI Aerogels at Different pH Values

			pseudo-second-order kinetic model		
sample	pH value	$Q_{e,exp}$ (%)	k_2 (h^{-1})	$Q_{e,cal}$ (%)	R^2
CNFs	7.4	91.07	0.938	91.24	0.9999
CNFs-PEI	2	59.53	0.007	64.31	0.9989
CNFs-PEI	7.4	86.32	0.008	92.59	0.9978

model with high correlation coefficients (R^2 = 0.9979−0.9999). In addition, the drug release from CNFs-PEI was highly pH-dependent. When in SGF (pH = 2), the cumulative drug release of CNFs-PEI was only 64.31%. However, when in SIF (pH = 7.4), it reached 92.59% with a much faster release rate. These results demonstrate a remarkable pH responsiveness of the CNF-PEI aerogel.[64,65] For clinical practices, the CNFs-PEI aerogels could slow down the initial burst release of NaSA in stomach and bring more drugs to the intestinal tract for a targeted drug delivery. This would not only reduce the side effects on stomach but also improve the absorption efficiency of drugs.[66] In addition to the above two different pH for the evaluation of drug release in SGF and SIF, pH 5 and 9 were also tested and the results were presented in Figure S2 and Table S1 in the Supporting Information.

Effect of Temperature on Drug Release. The drug release behaviors of CNFs-PEI aerogel were also examined at different temperatures in SIF (pH = 7.4). As shown in Figure 9a, the temperature of fluid could strongly affect the drug release. When the temperature rose up from 20 to 50 °C, the cumulative drug release increased from 52.66% to 78.49% (Table 4). The release rate also increased obviously. These results suggested that the desorption of NaSA was an endothermic process, and higher temperatures favored the drug release. Moreover, the molecule diffusion rate would increase at a higher temperature, which might lead to a faster drug release rate.[67] The NaSA release data at different temperatures were further analyzed using the pseudo-second-order kinetics model. The kinetics studies could help understand the drug release process in a particular environment and guide the dosage of drug carriers for oral administration.[68] The graphical representations and the corresponding parameters calculated from the kinetics model are shown in Figure 9b and Table 4, respectively. At all temperatures, the pseudo-second-order model provided a good fit to the kinetics data with high correlation coefficients (R^2 = 0.9782−0.9990). Because some disease states manifest themselves by a change in temperature,[69] the CNFs-PEI aerogels with a sensitive

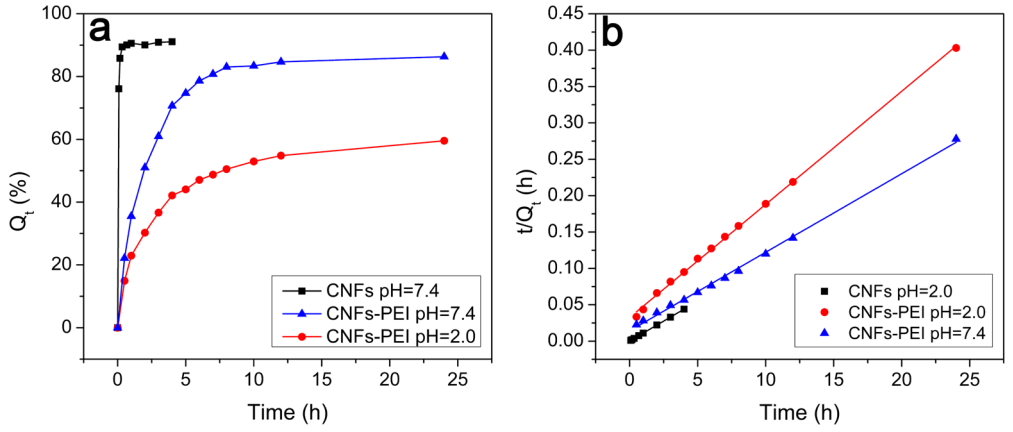

Figure 8. (a) NaSA cumulative release curves with time and (b) pseudo-second-order fitting on NaSA release data from CNFs and CNFs-PEI aerogels at various pH.

DOI: 10.1021/am507601m
ACS Appl. Mater. Interfaces 2015, 7, 2607−2615

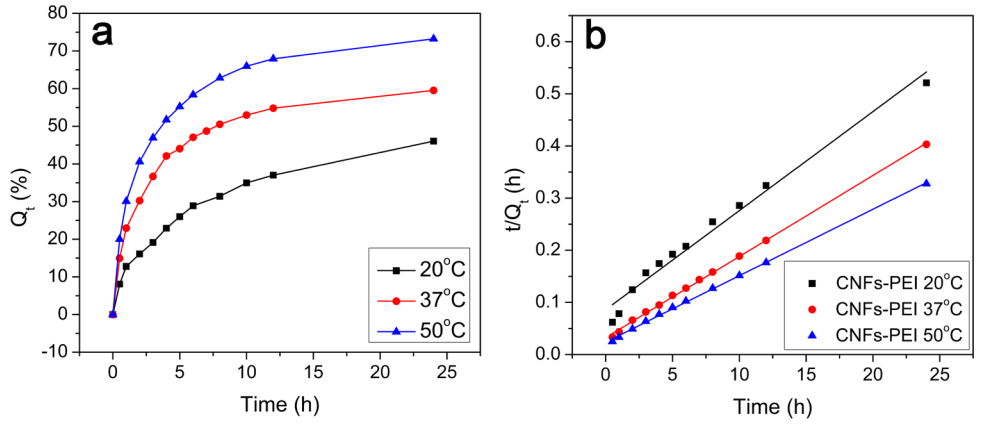

Figure 9. (a) NaSA cumulative release curves with time and (b) pseudo-second-order fitting on NaSA release data from CNFs-PEI aerogel at various temperatures.

Table 4. NaSA Release Kinetics from the Drug-Loaded CNFs-PEI Aerogels at Different Temperatures

		pseudo-second-order kinetic model		
temperature (°C)	$Q_{e,exp}$ (%)	k_2 (h^{-1})	$Q_{e2,cal}$ (%)	R^2
20	46.05	0.004	52.66	0.9782
37	59.53	0.007	64.31	0.9989
50	73.25	0.007	78.49	0.9990

temperature-responsive drug release behavior may open up opportunities to construct a novel drug delivery system in conjunction with localized hyperthermia. This strategy could achieve temporal drug delivery control: drug expresses its activity for a time period defined by local temperature change.[70]

CONCLUSION

In the present study, PEI modified CNFs aerogels were successfully developed as an alternative biopolymer-based drug delivery system to substitute the conventional synthetic ones. The aerogels were highly porous, bearing abundant of functional groups. The NaSA loading capability of CNFs-PEI aerogels was extraordinary. The maximum NaSA loading could be as high as 287.39 mg/g at pH 3, significantly higher than that of CNFs aerogels. The drug adsorption process followed Langmuir isotherm and pseudo-second-order kinetics model. Drug release studies indicated that the CNFs-PEI aerogels exhibited remarkable sustained drug release behaviors. More interestingly, both pH and temperature were discovered to affect the drug release profoundly, demonstrating strong controlled release behaviors of this drug carrier. It was envisaged that the simple fabricating process, the high drug loading capability, and the controlled drug release performance, together with the intrinsic nature of biodegradability and biocompatibility of cellulose, would make the CNFs-PEI aerogels a promising candidate for future pharmaceutical industries.

ASSOCIATED CONTENT

Supporting Information

The morphology of the CNFs-PEI aerogel after drug release and the study of drug release behavior under other pH values (5 and 9). This material is available free of charge via the Internet at http://pubs.acs.org.

AUTHOR INFORMATION

Corresponding Authors

*For W.Z.: phone/fax, (+086) 28-5460607; E-mail, weizhang@scu.edu.cn.

*For X.Z.: E-mail, zhangximu1212@163.com.

Notes

The authors declare no competing financial interest.

ACKNOWLEDGMENTS

We thank the National Natural Science Foundation of China (51303112, 51473100 and 51433006) for financial support of this work.

REFERENCES

(1) McCarthy, D. M. Comparative Toxicity of Nonsteroidal Anti-Inflammatory Drugs. *Am. J. Med.* **1999**, *107*, 37−46.

(2) Gabriel, S. E.; Jaakkimainen, L.; Bombardier, C. Risk for Serious Gastrointestinal Complications Related to Use of Nonsteroidal Anti-inflammatory Drugs−A Meta-analysis. *Ann. Int. Med.* **1991**, *115*, 787−796.

(3) Polisson, R. Nonsteroidal Anti-Inflammatory Drugs: Practical and Theoretical Considerations in Their Selection. *Am. J. Med.* **1996**, *100*, 31S−36S.

(4) Wang, N.; Wu, C.; Cheng, Y.; Xu, T. Organic−Inorganic Hybrid Anion Exchange Hollow Fiber Membranes: A Novel Device for Drug Delivery. *Int. J. Pharm.* **2011**, *408*, 39−49.

(5) Uhrich, K. E.; Cannizzaro, S. M.; Langer, R. S. Polymeric Systems for Controlled Drug Release. *Chem. Rev.* **1999**, *99*, 3181−3198.

(6) Bhosale, S. V.; Bhosale, S. V. Yoctowells as a simple model system for the encapsulation and controlled release of bioactive molecules. *Sci. Rep.* **2013**, *22*, 1982−1990.

(7) Li, Z.; Barnes, J. C.; Bosoy, A.; Stoddart, J. F.; Zink, J. I. Mesoporous silica nanoparticles in biomedical applications. *Chem. Soc. Rev.* **2012**, *41*, 2590−2605.

(8) Theron, C.; Gallud, A.; Carcel, C.; Gary-Bobo, M.; Maynadier, M.; Garcia, M.; Lu, J.; Tamanoi, F.; Zink, J. I.; Wong Chi Man, M. Hybrid Mesoporous Silica Nanoparticles with pH-Operated and Complementary H-Bonding Caps as an Autonomous Drug-Delivery System. *Chem.—Eur. J.* **2014**, *20*, 9372−9380.

(9) Okuda, T.; Tominaga, K.; Kidoaki, S. Time-programmed dual release formulation by multilayered drug-loaded nanofiber meshes. *J. Controlled Release* **2010**, *143*, 258−264.

(10) Cardamone, K.; Lofthouse, S. A.; Lucas, J. C.; Lee, R. P.; O'Donoghue, M.; Brandon, M. R. J. In Vitro Testing of a Pulsatile Delivery System and Its in Vivo Application for Immunisation Against Tetanus Toxoid. *J. Controlled Release* **1997**, *47*, 205−219.

DOI: 10.1021/am507601m
ACS Appl. Mater. Interfaces 2015, 7, 2607−2615

(11) Sintzel, M. B.; Bernatchez, S. F.; Tabatabay, C.; Gurny, R. Biomaterials in Ophthalmic Drug Delivery. *Eur. J. Pharm. Biopharm.* **1996**, *42*, 358−374.
(12) García-González, C. A.; Alnaief, M.; Smirnova, I. Polysaccharide-Based Aerogels—Promising Biodegradable Carriers for Drug Delivery Systems. *Carbohydr. Polym.* **2011**, *86*, 1425−1438.
(13) Cranston, E. D.; Eita, M.; Johansson, E.; Netrval, J.; Salajkova, M.; Arwin, H.; Wagberg, L. Determination of Young's Modulus for Nanofibrillated Cellulose Multilayer Thin Films Using Buckling Mechanics. *Biomacromolecules* **2011**, *12*, 961−969.
(14) Cranston, E. D.; Gray, D. G.; Rutland, M. W. Direct Surface force Measurements of Polyelectrolyte Multilayer Films Containing Nanocrystalline Cellulose. *Langmuir* **2010**, *26*, 17190−17197.
(15) Kumar, A.; Negi, Y. S.; Choudhary, V.; Bhardwaj, N. K. Microstructural and Mechanical Properties of Porous Biocomposite Scaffolds Based on Polyvinyl Alcohol, Nano-Hydroxyapatite and Cellulose Nanocrystals. *Cellulose* **2014**, *21*, 3409−3426.
(16) Ma, H.; Burger, C.; Hsiao, B. S.; Chu, B. Ultra-Fine Cellulose Nanofibers: New Nano-scale Materials for Water Purification. *J. Mater. Chem.* **2011**, *21*, 7507−7510.
(17) Siró, I.; Plackett, D.; Hedenqvist, M.; Ankerfors, M.; Lindström, T. Highly Transparent Films from Carboxymethylated Microfibrillated Cellulose: The Effect of Multiple Homogenization Steps on Key Properties. *J. Appl. Polym. Sci.* **2011**, *119*, 2652−2660.
(18) Pääkkö, M.; Ankerfors, M.; Kosonen, H.; Nykänen, A.; Ahola, S.; Österberg, M.; Ruokolainen, J.; Laine, J.; Larsson, P. T.; Ikkala, O.; Lindström, T. Enzymatic Hydrolysis Combined with Mechanical Shearing and High-Pressure Homogenization for Nanoscale Cellulose Fibrils and Strong Gels. *Biomacromolecules* **2007**, *8*, 1934−1941.
(19) Kumar, A.; Negi, Y. S.; Choudhary, V.; Bhardwaj, N. K. Characterization of Cellulose Nanocrystals Produced by Acid-Hydrolysis from Sugarcane Bagasse as Agro-waste. *J. Nonlinear Opt. Phys.* **2014**, *2*, 1−8.
(20) Yang, X.; Cranston, E. D. Chemically Cross-Linked Cellulose Nanocrystal Aerogels with Shape Recovery and Superabsorbent Properties. *Chem. Mater.* **2014**, *26*, 6016−6025.
(21) Kolakovic, R. *Nanofibrillar Cellulose in Drug Delivery*. Ph.D. Thesis. University of Helsinki, Helsinki, Finland, 2013.
(22) Kolakovic, R.; Laaksonen, T.; Peltonen, L.; Laukkanen, A.; Hirvonen, J. Spray-Dried Nanofibrillar Cellulose Microparticles for Sustained Drug Release. *Int. J. Pharm.* **2012**, *430*, 47−55.
(23) Bhattacharya, M.; Malinen, M. M.; Lauren, P.; Lou, Y.-R.; Kuisma, S. W.; Kanninen, L.; Lille, M.; Corlu, A.; GuGuen-Guillouzo, C.; Ikkala, O.; Laukkanen, A.; Urtti, A.; Yliperttul, M. Nanofibrillar Cellulose Hydrogel Promotes Three-Dimensional Liver Cell Culture. *J. Controlled Release* **2012**, *164*, 291−298.
(24) Kolakovic, R.; Peltonen, L.; Laukkanen, A.; Hirvonen, J.; Laaksonen, T. Nanofibrillar Cellulose Films for Controlled Drug Delivery. *Eur. J. Pharm. Biopharm.* **2012**, *82*, 308−315.
(25) Kolakovic, R.; Peltonen, L.; Laukkanen, A.; Hellman, M.; Laaksonen, P.; Linder, M. B.; Hirvonen, J.; Laaksonen, T. Evaluation of Drug Interactions with Nanofibrillar Cellulose. *Eur. J. Pharm. Biopharm.* **2013**, *85*, 1238−1244.
(26) Mohd Amin, M. C. I.; Ahmad, N.; Halib, N.; Ahmad, I. Synthesis and Characterization of Thermo-and pH-Responsive Bacterial Cellulose/Acrylic Acid Hydrogels for Drug Delivery. *Carbohydr. Polym.* **2012**, *88*, 465−473.
(27) Valo, H.; Arola, S.; Laaksonen, P.; Torkkeli, M.; Peltonen, L.; Linder, M. B.; Serimaa, R.; Kuga, S.; Hirvonen, J.; Laaksonen, T. Drug Release from Nanoparticles Embedded in Four Different Nanofibrillar Cellulose Aerogels. *Eur. J. Pharm. Sci.* **2013**, *50*, 69−77.
(28) Guenther, U.; Smirnova, I.; Neubert, R. H. H. Hydrophilic Silica Aerogels as Dermal Dug Delivery Systems—Dithranol as a Model Drug. *Eur. J. Pharm. Biopharm.* **2008**, *69*, 935−942.
(29) Moreno-Castilla, C.; Maldonado-Hódar, F. J. Carbon Aerogels for Catalysis Applications: An Overview. *Carbon* **2005**, *43*, 455−465.
(30) Mehling, T.; Smirnova, I.; Guenther, U.; Neubert, R. H. H. Polysaccharide-Based Aerogels as Drug Carriers. *J. Non-Cryst. Solids* **2009**, *355*, 2472−2479.
(31) Pääkkö, M.; Vapaavuori, J.; Silvennoinen, R.; Kosonen, H.; Ankerfors, M.; Lindström, T.; Berglund, L. A.; Ikkala, O. Long and Entangled Native Cellulose I Nanofibers Allow Flexible Aerogels and Hierarchically Porous Templates for Functionalities. *Soft Matter* **2008**, *4*, 2492−2499.
(32) Chen, W.; Li, Q.; Wang, Y.; Yi, X.; Zeng, J.; Yu, H.; Liu, Y.; Li, J. Comparative Study of Aerogels Obtained from Differently Prepared Nanocellulose Fibers. *ChemSusChem* **2014**, *7*, 154−161.
(33) Rodríguez, R.; Alvarez-Lorenzo, C.; Concheiro, A. Cationic Cellulose Hydrogels: Kinetics of the Cross-Linking Process and Characterization as pH-/Ion-Sensitive Drug Delivery Systems. *J. Controlled Release* **2003**, *86*, 253−265.
(34) Butun, S.; Ince, F. G.; Erdugan, H.; Sahiner, N. One-Step Fabrication of Biocompatible Carboxymethyl Cellulose Polymeric Particles for Drug Delivery Systems. *Carbohydr. Polym.* **2011**, *86*, 636−643.
(35) Patri, A. K.; Kukowska-Latallo, J. F.; Baker, J. R., Jr. Targeted Drug Delivery with Dendrimers: Comparison of the Release Kinetics of Covalently Conjugated Drug and Non-covalent Drug Inclusion Complex. *Adv. Drug. Delivery Rev.* **2005**, *57*, 2203−2214.
(36) Liu, B.; Huang, Y. Polyethyleneimine Modified Eggshell Membrane as a Novel Biosorbent for Adsorption and Detoxification of Cr (VI) from Water. *J. Mater. Chem.* **2011**, *21*, 17413−17418.
(37) Xia, T.; Kovochich, M.; Liong, M.; Meng, H.; Kabehie, S.; George, S.; Zink, J. I.; Nel, A. E. Polyethyleneimine Coating Enhances the Cellular Uptake of Mesoporous Silica Nanoparticles and Allows Safe Delivery of siRNA and DNA Constructs. *ACS Nano* **2009**, *3*, 3273−3286.
(38) Chertok, B.; David, A. E.; Yang, V. C. Polyethyleneimine-Modified Iron Oxide Nanoparticles for Brain Tumor Drug Delivery Using Magnetic Targeting and Intra-carotid Administration. *Biomaterials* **2010**, *31*, 6317−6324.
(39) Roseborough, I. E.; Grevious, M. A.; Lee, R. C. Prevention and Treatment of Excessive Dermal Scarring. *J. Int. Med. Res.* **2004**, *96*, 108−116.
(40) Hosny, E. A.; Al-Shora, H. I.; Elmazar, M. M.A. Oral Delivery of Insulin from Enteric-Coated Capsules Containing Sodium Salicylate: Effect on Relative Hypoglycemia of Diabetic Beagle Dogs. *Int. J. Pharm.* **2002**, *237*, 71−76.
(41) Ouimet, M. A.; Snyder, S. S.; Uhrich, K. E. Tunable Drug Release Profiles from Salicylate-Based Poly (Anhydride-Ester) Matrices Using Small Molecule Admixtures. *J. Bioact. Compat. Polym.* **2012**, *27*, 540−549.
(42) Wu, K. K. Aspirin and Salicylate An Old Remedy With a New Twist. *Circulation* **2000**, *102*, 2022−2023.
(43) Chung, Y. M.; Bae, Y. S.; Lee, S. Y. Molecular Ordering of ROS Production, Mitochondrial Changes, and Caspase Activation during Sodium Salicylate-Induced Apoptosis. *Free Radical Biol. Med.* **2003**, *34*, 434−442.
(44) Brunaue, S.; Emmet, P. H.; Tell, E. Adsorption of Gases in Multimolecular Layers. *J. Am. Chem. Soc.* **1938**, *60*, 309−319.
(45) Zhang, W.; Zhang, Y.; Lu, C.; Deng, Y. Aerogels from Crosslinked Cellulose Nano/Micro-Fibrils and Their Fast Shape Recovery Property in Water. *J. Mater. Chem.* **2012**, *22*, 11642−11650.
(46) Newcombe, G.; Hayesb, R.; Drikas, M. Granular activated carbon: importance of surface properties in the adsorption of naturally occurring organics. *Colloid. Surf., A* **1993**, *78*, 65−71.
(47) Zhang, Q.; Wang, N.; Xu, T.; Cheng, Y. Poly (Amidoamine) Dendronized Hollow Fiber Membranes: Synthesis, Characterization, and Preliminary Applications as Drug Delivery Devices. *Acta Biomater.* **2012**, *8*, 1316−1322.
(48) Wang, J.; Zhao, L.; Duan, W.; Han, L.; Chen, Y. Adsorption of Aqueous Cr(VI) by Novel Fibrous Adsorbent with Amino and Quaternary Ammonium Groups. *Ind. Eng. Chem. Res.* **2012**, *51*, 13655−13662.
(49) Han, K. N.; Yu, B. Y.; Kwak, S. Y. Hyperbranched Poly (Amidoamine)/Polysulfone Composite Membranes for Cd(II) Removal from Water. *J. Membr. Sci.* **2012**, *396*, 83−91.

DOI: 10.1021/am507601m
ACS Appl. Mater. Interfaces 2015, 7, 2607−2615

(50) Pan, B.; Gao, F.; Gu, H. Dendrimer Modified Magnetite Nanoparticles for Protein Immobilization. *J. Colloid Interface Sci.* **2005**, *284*, 1−6.
(51) Swartz, W. E. X-ray Photoelectron Spectroscopy. *Anal. Chem.* **1973**, *45*, 788a−800a.
(52) Matuana, L. M.; Balatinecz, J. J.; Sodhi, R. N. S.; Park, C. B. Surface Characterization of Esterified Cellulosic Fibers by XPS and FTIR Spectroscopy. *Wood Sci. Technol.* **2001**, *35*, 191−201.
(53) Po, H. N.; Senozan, N. M. The Henderson−Hasselbalch Equation: Its History and Limitations. *J. Chem. Educ.* **2001**, *78*, 1499−1503.
(54) Shapira, A.; Assaraf, Y. G.; Epstein, D.; Livney, Y. D. Beta-Casein Nanoparticles as an Oral Delivery System for Chemotherapeutic Drugs: Impact of Drug Structure and Properties on Co-assembly. *Pharm. Res.* **2010**, *27*, 2175−2186.
(55) Ungell, A.-L.; Nylander, S.; Bergstrand, S.; Sjoberg, A.; Enneras, H. L. Membrane Transport of Drugs in Different Regions of the Intestinal Tract of the Rat. *J. Pharm. Sci.* **1998**, *87*, 360−366.
(56) Amara, M.; Kerdjoudj, H. Modification of cation-exchange membrane properties by electro-adsorption of polyethyleneimine. *Desalination* **2003**, *155*, 79−87.
(57) Dbus, I. G.; Barriuso, E.; Calvet, R. Sorption of Weak Organic Acids in Soils: Clofencet, 2,4-D and Salicylic Acid. *Chemosphere* **2001**, *45*, 767−774.
(58) Langmuir, I. The Adsorption of Gases on Plane Surfaces of Glass, Mica and Platinum. *J. Am. Chem. Soc.* **1918**, *40*, 1361−1403.
(59) Dada, A. O.; Olalekan, A. P.; Olatunya, A. M.; Dada, O. Langmuir, Freundlich, Temkin and Dubinin−Radushkevich isotherms studies of equilibrium sorption of Zn^{2+} unto phosphoric acid modified rice husk. *J. Appl. Chem.* **2012**, *3*, 38−45.
(60) Tao, A.; Kim, F.; Hess, C.; Goldberger, J.; He, R.; Sun, Y.; Xia, Y.; Yang, P. Langmuir−Blodgett Silver Nanowire Monolayers for Molecular Sensing Using Surface Enhanced Raman Spectroscopy. *Nano Lett.* **2003**, *3*, 1229−1233.
(61) Shen, H.; Pan, S.; Zhang, Y.; Huang, X.; Gong, H. A New Insight on the Adsorption Mechanism of Amino-Functionalized Nano-Fe_3O_4 Magnetic Polymers in Cu(II), Cr(VI) Co-Existing Water System. *Chem. Eng. J.* **2012**, *183*, 180−191.
(62) Cook, R. O.; Pannu, R. K.; Kellaway, I. W. Novel sustained release microspheres for pulmonary drug delivery. *J. Controlled Release* **2005**, *104*, 79−90.
(63) Yuan, X.; Xing, W.; Zhuo, S.; Han, Z.; Wang, G.; Gao, X.; Yan, Z. Preparation and Application of Mesoporous Fe/Carbon Composites as a Drug Carrier. *Microporous Mesoporous Mater.* **2009**, *117*, 678−684.
(64) Theron, C.; Gallud, A.; Carcel, C.; Gary-Bobo, M.; Maynadier, M.; Garcia, M.; Lu, J.; Tamanoi, F.; Zink, J. I.; Wong Chi Man, M. Hybrid Mesoporous Silica Nanoparticles with pH-Operated and Complementary H-Bonding Caps as an Autonomous Drug-Delivery System. *Chem.—Eur. J.* **2014**, *20*, 9372−9380.
(65) Okuda, T.; Tominaga, K.; Kidoaki, S. Time-programmed dual release formulation by multilayered drug-loaded nanofiber meshes. *J. Controlled Release* **2010**, *143*, 258−264.
(66) Mitchell, J. A.; Akarasereenont, P.; Thiemermann, C.; Flower, R. J.; Vane, J. R. Selectivity of Nonsteroidal Antiinflammatory Drugs as Inhibitors of Constitutive and Inducible Cyclooxygenase. *Proc. Natl. Acad. Sci. U. S. A.* **1993**, *90*, 11693−11697.
(67) Kost, J.; Langer, R. Responsive Polymeric Delivery Systems. *Adv. Drug. Delivery Rev.* **2012**, *64*, 327−341.
(68) Patri, A. K.; Kukowska-Latallo, J. F.; Baker, J. R. Targeted Drug Delivery with Dendrimers: Comparison of the Release Kinetics of Covalently Conjugated Drug and Non-covalent Drug Inclusion Complex. *Adv. Drug. Delivery Rev.* **2005**, *57*, 2203−2214.
(69) Zhang, L.; Xu, T.; Lin, Z. Controlled Release of Ionic Drug through the Positively Charged Temperature-Responsive Membranes. *J. Membr. Sci.* **2006**, *281*, 491−499.
(70) Chung, J. E.; Yokoyama, M.; Yamato, M.; Aoyagi, T.; Sakurai, Y.; Okano, T. Thermo-Responsive Drug Delivery from Polymeric Micelles Constructed Using Block Copolymers of Poly(*N*-isopropylacrylamide) and Poly(Butylmethacrylate). *J. Controlled Release* **1999**, *62*, 115−127.

DOI: 10.1021/am507601m
ACS Appl. Mater. Interfaces 2015, 7, 2607−2615